

Optimal Position and Velocity Navigation Filters with Discrete-Time Delayed Measurements

Pedro Batista, Carlos Silvestre, Paulo Oliveira

Abstract—This paper presents the design and performance evaluation of a continuous-time Kalman filter with discrete-time delayed measurements for a class of time-varying kinematic systems with application to the estimation of linear motion quantities, in three dimensions, of mobile platforms. The design is based on the Kalman filter solution for an equivalent linear time invariant realization and allows for the natural use of frequency weights to explicitly achieve adequate disturbance rejection and measurement noise attenuation on the state estimates. Moreover, the proposed solution is optimal with respect to all signals assuming exact angular measurements. Two applications in the field of ocean robotics are presented and simulation results are included that illustrate the achievable performance in the presence of both extreme environmental disturbances and realistic measurements, with noise and delays.

I. INTRODUCTION

The design of Navigation and Positioning Systems plays a key role in the development of a large variety of mobile platforms. Indeed, the quality of the navigation data is a fundamental requirement in many data acquisition applications and it is also necessary for control purposes, where other quantities such as the attitude of the vehicle and/or the linear and angular velocities are also often required. This paper presents the design and performance evaluation of a filter with discrete-time delayed measurements for a class of kinematic systems with application to the estimation of linear motion quantities in Integrated Navigation Systems for mobile platforms and, in particular, underwater vehicles.

To tackle this class of problems several approaches have been proposed in the literature. In [1] a GES nonlinear control law is presented for ships, in two-dimensions, which includes a nonlinear observer to provide the state of the vehicle. This observer relies on the vehicle dynamics but, as discussed in [2], it does not apply to unstable ships. In [2] a solution to an extended class of ships is proposed requiring only stable surge dynamics. In [3] a globally exponentially stable (GES) observer for ships (in two-dimensions) that includes features such as wave filtering and bias estimation is presented and in [4] an extension to this result with adaptive wave filtering is available. An alternative filter was proposed in [5] where the problem of estimating the velocity and position of an autonomous vehicle in three-dimensions was solved by resorting to special bilinear time-varying complementary filters. More recently, a pair of coworking

This work was partially supported by Fundação para a Ciência e a Tecnologia (ISR/IST pluriannual funding) and project MEDIRES from ADI through the POS_Conhecimento Program that includes FEDER funds, and by the project PDCT/MAR/55609/2004 - RUMOS of the FCT. The work of P. Batista was supported by a PhD Student Scholarship from the POCTI Programme of FCT, SFRH/BD/24862/2005.

The authors are with the Institute for Systems and Robotics, Instituto Superior Técnico, Av. Rovisco Pais, 1049-001 Lisboa, Portugal. {pbatista, cjs, pjcro}@isr.ist.utl.pt

nonlinear Luenberger GES observers for autonomous underwater vehicles (AUVs), in 3D, was proposed in [6], which also elaborates on the destabilizing Coriolis and centripetal forces and moments. However, this last approach assumes, among others, limited pitch angles. A more complete survey on the subject of underwater vehicle navigation can be found in [7]. General drawbacks of the above-mentioned results include the absence of systematic tuning procedures and the inherent limitations of the vehicle dynamic models, which are seldom known in full detail and may be subject to variations over time. Additionally, it is often assumed to have available continuous measurements, while that is not true for all sensors, particularly positioning sensors.

The main contribution of this paper is the design of a continuous-time Kalman filter with discrete-time delayed measurements for a class of time-varying kinematic systems with application to the estimation of linear motion quantities (position, linear velocity, ocean current, and acceleration of gravity), in three dimensions, in underwater robotics. At the core of the proposed methodology there is a time-varying orthogonal Lyapunov transformation that renders the dynamics of the kinematic system linear time invariant (LTI). This allows for the derivation of an equivalent continuous-time Kalman filter with discrete-time delayed measurements for the LTI realization, which is then converted back to the original space, yielding the final optimal filtering solution for the time-varying system. Frequency weights may be included in the design to explicitly achieve adequate disturbance rejection and measurement noise attenuation on the state estimates. Moreover, a filtering limit solution is presented which does not require the solution of a Lyapunov matrix differential equation each time a new measurement arrives. This is of great importance since it lessens the computational cost and allows for a straightforward digital implementation of the filter. Applications of the proposed filtering design technique are presented to estimate linear motion quantities in Integrated Navigation Systems for underwater vehicles. The vehicle tri-dimensional motion is described by pure kinematic models. This class of models, expressed in the inertial coordinate system, has been widely used by the Navigation community, see [8] and the references therein. The present solution departs from previous approaches as it considers the rigid-body kinematics expressed in body-fixed coordinates, which allows for the derivations presented in the paper. Moreover, the proposed solution is optimal with respect to all signals assuming exact angular measurements. This paper builds on previous work by the authors that can be found in [9] and [10] where Kalman and \mathcal{H}_∞ filters were derived for continuous-time kinematic systems with continuous-time measurements.

The paper is organized as follows. The class of dynamic

systems and the filter design are introduced in Section II, where a filtering limit solution and practical considerations are also referred. Two different applications are presented in Sections III and IV and simulation results are included that illustrate the achievable performance in the presence of both extreme environmental disturbances and realistic measurement noise. Finally, Section V summarizes the main contributions and conclusions of the paper.

Throughout the paper the symbol $\mathbf{0}_{n \times m}$ denotes an $n \times m$ matrix of zeros, \mathbf{I}_n an identity matrix with dimension $n \times n$, and $\text{diag}(\mathbf{A}_1, \dots, \mathbf{A}_n)$ a block diagonal matrix. When the dimensions are omitted the matrices are assumed of appropriate dimensions.

II. FILTER DESIGN

A. System Dynamics

Consider the class of dynamic systems

$$\begin{cases} \dot{\boldsymbol{\eta}}_p(t) = \mathbf{A}_p \boldsymbol{\eta}_p(t) - \mathbf{M}_S[\boldsymbol{\omega}(t)] \boldsymbol{\eta}_p(t) + \mathbf{B}_p(t) \boldsymbol{\tau}(t) + \mathbf{d}(t), \\ \boldsymbol{\psi}(t) = \mathbf{C}_p \boldsymbol{\eta}_p(t) + \mathbf{n}(t) \end{cases}, \quad (1)$$

where $\boldsymbol{\eta}_p(t) = [\boldsymbol{\eta}_1^T(t) \dots \boldsymbol{\eta}_N^T(t)]^T$, with $\boldsymbol{\eta}_i(t) \in X_i \subseteq \mathbb{R}^3$, $i = 1, \dots, N$, is the system state, $\boldsymbol{\psi}(t) \in \mathbb{R}^3$ is the system output, $\boldsymbol{\tau}(t)$ is a deterministic system input, $\mathbf{d}(t)$ denotes the system disturbances input, $\mathbf{n}(t)$ denotes a disturbance that affects the output of the system, not necessarily measurement noise, $\boldsymbol{\omega}(t) \in \mathbb{R}^3$ is a continuous bounded function of t , $\mathbf{M}_S[\boldsymbol{\omega}(t)]$ is the block diagonal matrix $\mathbf{M}_S[\boldsymbol{\omega}(t)] := \text{diag}(\mathbf{S}[\boldsymbol{\omega}(t)], \dots, \mathbf{S}[\boldsymbol{\omega}(t)])$, where $\mathbf{S}[\boldsymbol{\omega}(t)]$ is a skew-symmetric matrix that verifies $\mathbf{S}(\mathbf{a}) \mathbf{b} = \mathbf{a} \times \mathbf{b}$, with \times denoting the cross product, and that satisfies $\dot{\mathbf{R}}(t) = \mathbf{R}(t) \mathbf{S}[\boldsymbol{\omega}(t)]$, where $\mathbf{R}(t) \in \text{SO}(3)$, i.e., $\mathbf{R}(t)$ is a proper rotation matrix,

$$\mathbf{A}_p = \begin{bmatrix} \mathbf{0} & \gamma_1 \mathbf{I} & \mathbf{0} & \dots & \mathbf{0} \\ \vdots & \ddots & \ddots & \ddots & \vdots \\ \vdots & & \ddots & \ddots & \mathbf{0} \\ \vdots & & & \ddots & \vdots \\ \mathbf{0} & \dots & \dots & \dots & \gamma_{N-1} \mathbf{I} \\ & & & & \mathbf{0} \end{bmatrix},$$

$\gamma_i \in \mathbb{R}$, $\gamma_i \neq 0$, $i = 1, \dots, N-1$, and $\mathbf{C}_p = [\mathbf{I}_3 \mathbf{0} \dots \mathbf{0}]$. For design purposes consider that the disturbance input $\mathbf{d}(t)$ is given by $\mathbf{d}(t) := \mathbf{T}^T(t) \mathbf{L}_p \mathbf{d}(t)$, where $\mathbf{T}(t) := \text{diag}(\mathbf{R}(t), \dots, \mathbf{R}(t))$ and $\mathbf{d}(t)$ is the output of a stable LTI system \mathcal{W}_d driven by zero-mean, unit intensity white noise. Similarly, suppose that the disturbance that affects the output of the system is given by $\mathbf{n}(t) := \mathbf{R}^T(t) \mathbf{M}_p \mathbf{n}(t)$, where $\mathbf{n}(t)$ is the output of a stable LTI system \mathcal{W}_n also driven by zero-mean, unit intensity white noise. Further assume that \mathcal{W}_n is a strictly proper system. This is a mild assumption as in nature there are no processes with infinite energy. Finally, suppose that the output of the system is sampled at constant rate and that the measurements arrive with time-varying delays, as given by

$$\boldsymbol{\psi}_k^d = \boldsymbol{\psi}^d(t_k^d) = \boldsymbol{\psi}(t_k) + \mathbf{R}^T(t_k) \mathbf{n}_d(t_k), \quad k \in \mathbb{N},$$

where \mathbf{n}_d is discrete-time zero-mean white noise with covariance $N_d \mathbf{I}$, t_k^d denotes the instant of arrival of the measurement k , and t_k denotes the sampling instant of measurement k , given by $t_k = kT$, $k \in \mathbb{N}$, where T denotes the sampling period. A temporal diagram that illustrates the output sampling is depicted in Fig. 1. It is now clear why \mathcal{W}_n must be a strictly proper system, as if that was not the case, $\boldsymbol{\psi}(t)$ would contain white noise components that would

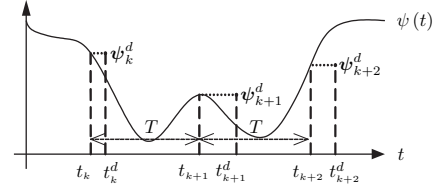


Fig. 1. Temporal Diagram

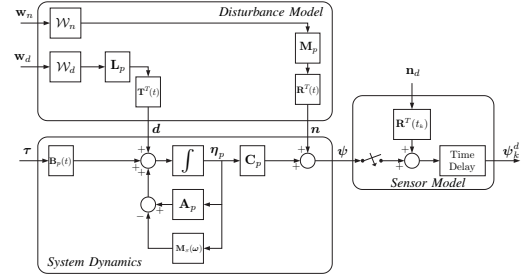


Fig. 2. Filter design setup

lead to a discrete sequence of measurements with infinite variance. Notice that the signal $\mathbf{n}_d^i(t_k) := \mathbf{R}^T(t_k) \mathbf{n}_d(t_k)$ is also zero-mean white noise and its covariance is the same of $\mathbf{n}_d(t_k)$. Thus, from the practical point of view, the rotation $\mathbf{R}^T(t_k)$ has no significant impact. However, it does simplify the final filter equations. The overall design setup is depicted in Fig. 2, where $\mathbf{w} = [\mathbf{w}_d^T \mathbf{w}_n^T]^T$ is zero-mean, unit intensity white noise.

Let $\mathbf{x}_d(t)$ and $\mathbf{x}_n(t)$ denote the internal states of state space realizations $(\mathbf{A}_d, \mathbf{B}_d, \mathbf{C}_d, \mathbf{D}_d)$ and $(\mathbf{A}_n, \mathbf{B}_n, \mathbf{C}_n, \mathbf{0})$ of \mathcal{W}_d and \mathcal{W}_n , respectively. Then, the augmented system dynamics can be written as

$$\begin{cases} \dot{\boldsymbol{\eta}}(t) = \mathbf{A}(t) \boldsymbol{\eta}(t) + \mathbf{B}_p(t) \boldsymbol{\tau}(t) + \mathbf{B}(t) \mathbf{w}(t) \\ \boldsymbol{\psi}_k^d = \mathbf{C}(t_k) \boldsymbol{\eta}(t_k) + \mathbf{R}^T(t_k) \mathbf{n}_d(t_k), \quad k \in \mathbb{N} \end{cases}, \quad (2)$$

where $\boldsymbol{\eta}(t) := [\boldsymbol{\eta}_p^T(t) \mathbf{x}_d^T \mathbf{x}_n^T]^T$,

$$\mathbf{A}(t) = \begin{bmatrix} \mathbf{A}_p - \mathbf{M}_S[\boldsymbol{\omega}(t)] & \mathbf{T}^T(t) \mathbf{L}_p \mathbf{C}_d & \mathbf{0} \\ \mathbf{0} & \mathbf{A}_d & \mathbf{0} \\ \mathbf{0} & \mathbf{0} & \mathbf{A}_n \end{bmatrix},$$

$$\mathbf{B}_p(t) = \begin{bmatrix} \mathbf{B}_p(t) \\ \mathbf{0} \\ \mathbf{0} \end{bmatrix}, \quad \mathbf{B}(t) = \begin{bmatrix} \mathbf{T}^T(t) \mathbf{L}_p \mathbf{C}_d & \mathbf{0} \\ \mathbf{B}_d & \mathbf{0} \\ \mathbf{0} & \mathbf{B}_n \end{bmatrix},$$

and $\mathbf{C}(t) = [\mathbf{C}_p \mid \mathbf{0} \mid \mathbf{R}^T(t) \mathbf{M}_p \mathbf{C}_n]$.

B. Filter Equations

In order to derive the optimal Kalman filter, consider the Lyapunov coordinate transformation proposed in [9] and define

$$\mathbf{x}(t) := \mathbf{T}_c(t) \boldsymbol{\eta}(t), \quad (3)$$

where $\mathbf{T}_c(t) := \text{diag}(\mathbf{T}(t), \mathbf{I}, \mathbf{I})$. Define also an equivalent output as

$$\mathbf{y}_k^d = \mathbf{R}(t_k) \boldsymbol{\psi}_k^d \quad (4)$$

Then, the dynamics of the system expressed in this new coordinate space can be written as

$$\begin{cases} \dot{\mathbf{x}}(t) = \mathbf{A} \mathbf{x}(t) + \mathbf{B} \mathbf{w}(t) + \mathbf{T}_c(t) \mathbf{B}_p(t) \boldsymbol{\tau}(t) \\ \mathbf{y}_k^d = \mathbf{C} \mathbf{x}(t_k) + \mathbf{n}_d(t_k), \quad k \in \mathbb{N} \end{cases}, \quad (5)$$

where

$$\mathbf{A} := \begin{bmatrix} \mathbf{A}_p & \mathbf{L}_p \mathbf{C}_d & \mathbf{0} \\ \mathbf{0} & \mathbf{A}_d & \mathbf{0} \\ \mathbf{0} & \mathbf{0} & \mathbf{A}_n \end{bmatrix}, \quad \mathbf{B} := \begin{bmatrix} \mathbf{L}_p \mathbf{D}_d & \mathbf{0} \\ \mathbf{B}_d & \mathbf{0} \\ \mathbf{0} & \mathbf{B}_n \end{bmatrix},$$

and $\mathbf{C} := \mathbf{R}(t_k) \mathbf{C}(t_k) \mathbf{T}_c^T(t_k) = [\mathbf{C}_p | \mathbf{0} | \mathbf{M}_p \mathbf{C}_n]$. The advantage of using these coordinate transformations is that the state dynamics become linear time invariant in what concerns the dependence on the state and the noise. The deterministic input is simply canceled out in the filter design.

The Kalman filter for the continuous-discrete system (5) is given by

$$\begin{cases} \dot{\hat{\mathbf{x}}}(t) = \mathbf{A}\hat{\mathbf{x}}(t) + \mathbf{T}_c(t)\mathbf{B}_p(t)\boldsymbol{\tau}(t), & t_k^d \leq t < t_{k+1}^d \\ \hat{\mathbf{x}}(t_k^d) = \hat{\mathbf{x}}(t_k^{d-}) + \boldsymbol{\Phi}(t_k^d, t_k)\mathbf{K}(t_k) [\mathbf{y}(t_k^d) - \mathbf{C}\hat{\mathbf{x}}(t_k)], \\ \hat{\mathbf{x}}(t_0) = \hat{\mathbf{x}}_0 = \mathbf{T}_c(t_0)\hat{\boldsymbol{\eta}}_0 \end{cases},$$

where $t_0^d = t_0$, $\hat{\boldsymbol{\eta}}_0$ is the initial state estimate, $\boldsymbol{\Phi}(t_k^d, t_k) = e^{\mathbf{A}(t_k^d - t_k)}$ is the transition matrix, and $\mathbf{K}(t_k)$ is the Kalman gain matrix, given by

$$\mathbf{K}(t_k) = \frac{1}{N_d} \mathbf{P}_c(t_k) \mathbf{C}^T,$$

where $\mathbf{P}_c(t)$ denotes the covariance of the error of the estimate of the state at time t assuming there are no measurement delays, whose dynamics are given by

$$\begin{cases} \dot{\mathbf{P}}_c(t) = \mathbf{A}\mathbf{P}_c(t) + \mathbf{P}_c(t)\mathbf{A}^T + \mathbf{B}\mathbf{B}^T, & t_{k-1} \leq t < t_k, k \in \mathbb{N} \\ \mathbf{P}_c(t_0) = \mathbf{P}_{c0} = \mathbf{T}_c(t_0)\mathbf{P}_{c0}\mathbf{T}_c^T(t_0) \end{cases},$$

where $\mathbf{P}_{c0} = \mathbf{P}_0 \succ \mathbf{0}$ is the initial covariance matrix and the discrete update at time t_k is given by

$$\mathbf{P}_c(t_k) = \mathbf{P}_c(t_k^-) - \mathbf{P}_c(t_k^-) \mathbf{C}^T \left[\mathbf{C}\mathbf{P}_c(t_k^-) \mathbf{C}^T + N_d \mathbf{I} \right]^{-1} \mathbf{C}\mathbf{P}_c(t_k^-). \quad (6)$$

The transition matrix simply propagates the discrete update to compensate for the measurements delays.

The filter equations in the original coordinate space can be recovered by inverting the coordinate transformations (3) and (4), which gives

$$\begin{cases} \dot{\hat{\boldsymbol{\eta}}}(t) = \mathbf{A}(t)\hat{\boldsymbol{\eta}}(t) + \mathbf{B}_p(t)\boldsymbol{\tau}(t), & t_{k-1}^d \leq t < t_k^d, k \in \mathbb{N} \\ \hat{\boldsymbol{\eta}}(t_k^d) = \hat{\boldsymbol{\eta}}(t_k^{d-}) + \boldsymbol{\Phi}(t_k^d, t_k)\mathbf{K}(t_k) [\boldsymbol{\psi}_k^d - \mathbf{C}(t_k)\hat{\boldsymbol{\eta}}(t_k)], \\ \hat{\boldsymbol{\eta}}(t_0) = \hat{\boldsymbol{\eta}}_0 \end{cases} \quad (7)$$

where $\boldsymbol{\Phi}(t_k^d, t_k)$ denotes the transition matrix associated with $\mathbf{A}(t)$, that can be written as

$$\boldsymbol{\Phi}(t_k^d, t_k) = \mathbf{T}_c^T(t_k^d) \boldsymbol{\Phi}(t_k^d, t_k) \mathbf{T}_c(t_k),$$

and $\mathbf{K}(t_k)$ is the Kalman gain matrix, given by

$$\mathbf{K}(t_k) = \mathbf{P}_c(t_k) \mathbf{C}^T(t_k), \quad (8)$$

where $\mathbf{P}_c(t)$ denotes the covariance matrix of the error of the estimate of $\boldsymbol{\eta}$ at time t if there were no measurement delays, which can be expressed as

$$\mathbf{P}_c(t) = \frac{1}{N_d} \mathbf{T}_c^T(t) \mathbf{P}_c(t) \mathbf{T}_c(t). \quad (9)$$

The following theorem summarizes the main result of this section.

Theorem 1: Consider the generalized system dynamics as depicted in Fig. 2, where $\mathbf{w} = [\mathbf{w}_d^T \mathbf{w}_n^T]^T$ is zero-mean, unit intensity, continuous-time white noise and \mathbf{n}_d is zero-mean, discrete-time white noise, with covariance matrix $N_d \mathbf{I}$. Assume that $\boldsymbol{\eta}(t_0)$, $\mathbf{w}(t)$ and $\mathbf{n}_d(t_k)$ are mutually

uncorrelated for all time. Let $t_0^d = t_0$, $\hat{\boldsymbol{\eta}}_0$ be the initial state estimate and \mathbf{P}_0 the initial error covariance matrix. Then, the optimal Kalman filter is given by (7) and the error covariance matrix $\mathbf{P}(t)$ can be expressed as

$$\mathbf{P}(t) = \mathbf{T}_c^T(t) \mathbf{P}(t) \mathbf{T}_c(t) \quad (10)$$

where $\mathbf{P}(t)$ satisfies

$$\begin{cases} \dot{\mathbf{P}}(t) = \mathbf{A}\mathbf{P}(t) + \mathbf{P}(t)\mathbf{A}^T + \mathbf{B}\mathbf{B}^T, & t_{k-1}^d \leq t < t_k^d, k \in \mathbb{N} \\ \mathbf{P}(t_0^d) = \mathbf{P}_0 \end{cases}, \quad (11)$$

and the discrete update is given by the propagation of $\mathbf{P}_c(t_k)$, which can be written as

$$\begin{aligned} \mathbf{P}(t_k^d) &= \mathbf{P}(t_k^{d-}) - \boldsymbol{\Phi}(t_k^d, t_k) \mathbf{P}(t_k) \mathbf{C}^T \\ &\quad \left[\mathbf{C}\mathbf{P}(t_k) \mathbf{C}^T + \mathbf{I} \right]^{-1} \mathbf{C}\mathbf{P}(t_k) \boldsymbol{\Phi}^T(t_k^d, t_k), \quad k \in \mathbb{N}. \end{aligned} \quad (12)$$

Proof: The Kalman filter dynamics (7) are standard, where $\boldsymbol{\Phi}(t_k^d, t_k)$ accounts for the correction due to the measurement delays. To show that the Kalman gain is given by (8) it remains to show that (9) is the solution of

$$\dot{\mathbf{P}}_c(t) = \mathbf{A}(t)\mathbf{P}_c(t) + \mathbf{P}_c(t)\mathbf{A}^T(t) + \mathbf{B}(t)\mathbf{B}^T(t), \quad t_{k-1} \leq t < t_k, k \in \mathbb{N}, \quad (13)$$

with $\mathbf{P}_c(t_0) = \mathbf{P}_{c0}$ and

$$\mathbf{P}_c(t_k) = \mathbf{P}_c(t_k^-) - \mathbf{P}_c(t_k^-) \mathbf{C}^T \left[\mathbf{C}(t_k) \mathbf{P}_c(t_k^-) \mathbf{C}^T(t_k) + N_d \mathbf{I} \right]^{-1} \mathbf{C}(t_k) \mathbf{P}_c(t_k^-). \quad (14)$$

Substituting (6) in (9) immediately yields (14). After a few algebraic manipulations, the time derivative of (9) gives (13). The actual error covariance matrix does not coincide with $\mathbf{P}_c(t)$ due to the measurement delays. Thus, between arrivals of the measurements, the covariance matrix is integrated in open-loop according to (11) and at the time of arrival t_k^d , the covariance is updated so that it coincides with $\mathbf{P}_c(t_k^d)$, i.e., $\mathbf{P}(t_k^d) = \mathbf{P}_c(t_k^d)$. It is a simple matter to show that (10) verifies these conditions. ■

C. Filtering Limit Solution

In the previous section the filter equations were derived by means of appropriate Lyapunov transformations that rendered the dynamics linear time invariant, as given by (5). Under appropriate stabilizability and detectability hypothesis, it is well known that the Kalman filter for the continuous-discrete LTI system (5) converges to an asymptotically stable steady-state solution. The existence of a special relationship between (5) and (2) induces a limit filtering solution for the system at hand.

Define $\bar{\boldsymbol{\Phi}} := \boldsymbol{\Phi}(T, 0)$,

$$\mathbf{Q} := \int_0^T \boldsymbol{\Phi}(T, \tau) \mathbf{B}\mathbf{B}^T \boldsymbol{\Phi}^T(T, \tau) d\tau,$$

and suppose that the pairs $(\bar{\boldsymbol{\Phi}}, \mathbf{Q})$ and $(\bar{\boldsymbol{\Phi}}, \mathbf{C})$ are stabilizable and detectable, respectively. Notice that this only depends on the proper choice of the filters \mathcal{W}_d and \mathcal{W}_n , as well as the matrices \mathbf{L}_p and \mathbf{M}_p . Under these conditions the estimation error covariance matrix $\mathbf{P}_c(t_k)$ converges to

$$\lim_{k \rightarrow \infty} \mathbf{P}_c(t_k) = \mathbf{P}_c^\infty, \quad (15)$$

with $\mathbf{P}_c^\infty := \mathbf{P}_c^r - \mathbf{P}_c^r \mathbf{C}^T (\mathbf{C}\mathbf{P}_c^r \mathbf{C}^T + N_d \mathbf{I})^{-1} \mathbf{C}\mathbf{P}_c^r$, where \mathbf{P}_c^r is the solution of the discrete-time algebraic Riccati equation

$$\mathbf{P}_c^r = \bar{\boldsymbol{\Phi}} \mathbf{P}_c^r \bar{\boldsymbol{\Phi}}^T + \mathbf{Q} - \bar{\boldsymbol{\Phi}} \mathbf{P}_c^r \mathbf{C}^T [\mathbf{C}\mathbf{P}_c^r \mathbf{C}^T + N_d \mathbf{I}]^{-1} \mathbf{C}\mathbf{P}_c^r \bar{\boldsymbol{\Phi}}^T.$$

From (8), (9), and (15) it follows that the Kalman gain converges to the limit solution

$$\lim_{k \rightarrow \infty} \mathcal{K}(t_k) = \mathbf{T}_c^T(t_k) \mathbf{P}_c^\infty \mathbf{T}_c(t_k) \mathbf{C}^T(t_k). \quad (16)$$

The Kalman filter that results from using the limit solution for the gain (16) is still time-varying due to the inherent nature of the system dynamics. However, the gain is now readily obtained and does not require the solution of a Lyapunov matrix differential equation, which could be computationally expensive.

D. Implementation

This section refers to some practical considerations regarding the implementation of the proposed filter. Figure 3 presents the block diagram implementation of the proposed solution, where the dashed lines represent injection of initial conditions on the various blocks each time a new measurement is available. Although the system dynamics presented in the paper are continuous, it turns out, in practice, that the filter is implemented in a discrete-time framework. Thus, the open-loop propagation of the system state estimate is executed resorting to integration algorithms such as Runge-Kutta methods. The signals ω , \mathbf{R} , and τ are thus sampled at high rates in order to allow accurate numerical integration of the state estimate.

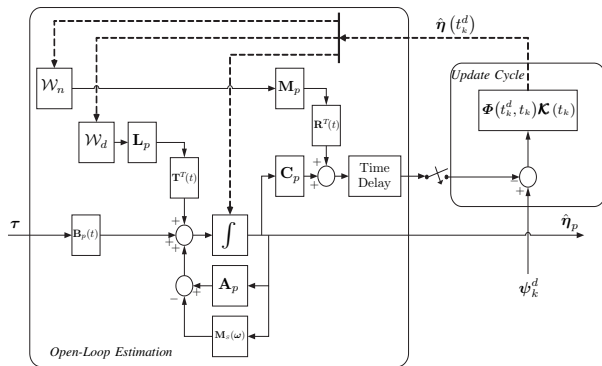


Fig. 3. Block Diagram of the Filter Implementation

III. POSITION AND OCEAN CURRENT VELOCITY NAVIGATION FILTER

In [10] a filtering solution is presented to obtain an estimate of the velocity of a constant unknown ocean current. The filter is not only globally exponentially stable but also optimal with respect to disturbances and measurement noise assuming exact angular measurements. The drawback of the solution is that it requires continuous-time measurements, which are not available in practice. This section revisits and successfully addresses this problem resorting to the theoretical results proposed in Section II. The proposed filtering framework is presented in Section III-A, whereas simulation results are detailed in Section III-B.

A. Filtering Framework

Consider an autonomous underwater vehicle equipped with a Doppler velocity log, which measures the velocity of the vehicle relative to the water, expressed in body-fixed coordinates, and an Attitude and Heading Reference System

(AHRS), which provides both the attitude and angular velocity of the vehicle, expressed in body-fixed coordinates. These two sensors do not require any external devices and provide high data rate signals. Moreover, in shallow waters, the Doppler velocity log can also be used to measure the velocity of the vehicle relative to the inertial frame and that would allow the indirect measurement of the velocity of the ocean current, since $\mathbf{v}(t) = \mathbf{v}_r(t) + \mathbf{v}_c(t)$, where \mathbf{v}_r and \mathbf{v} denote the relative and inertial velocity of the vehicle, respectively, and \mathbf{v}_c represents the ocean current velocity, all expressed in body-fixed coordinates. However, when the AUV is moving far away from the seabed, the inertial velocity is unavailable. Thus, an alternative strategy is required. The filter proposed in this section requires an acoustic positioning system, like an Ultra Short Baseline (USBL) sensor, that provides the position relative to the vehicle of a buoy moored in the mission scenario, where an acoustic transponder is installed. It is assumed that the USBL samples the position of the buoy with constant period and that the measure is available only after a variable time delay due to processing requirements.

Let $\mathbf{e}(t)$ denote the position of the buoy relative to the vehicle and expressed in body-fixed coordinates, as measured by the USBL. Its time derivative is given by

$$\dot{\mathbf{e}}(t) = -\mathbf{v}_r(t) - \mathbf{v}_c(t) - \mathbf{S}[\omega(t)] \mathbf{e}(t). \quad (17)$$

Since the ocean current is assumed constant in inertial coordinates the time derivative of $\mathbf{v}_c(t)$ can be written as

$$\dot{\mathbf{v}}_c(t) = -\mathbf{S}[\omega(t)] \mathbf{v}_c(t). \quad (18)$$

Clearly, the dynamics (17)-(18) fit in the class of systems (1) proposed in the paper. The usefulness of the frequency weights becomes more clear now. The buoy, moored in the mission scenario, is naturally subject to the sea waves, whose spectral density is approximately known. The effect of the waves on the buoy may be considered as disturbances in the output and thus modeled by the output frequency weight \mathcal{W}_n . Moreover, it turns out that these disturbances are modeled in the correct space, in spite of the fact that the filter works in body-fixed coordinates whereas the model for the sea waves exists in inertial coordinates. This is due to the inverse rotation matrix included for design purposes on the disturbances affecting the system output, see Fig. 2.

B. Simulation Results

In order to evaluate the performance achieved with the proposed filtering solution simulations were carried out with a simplified model of the SIRENE underwater vehicle, see [11]. The trajectory described by the vehicle is shown in Fig. 4, where the undisturbed position of the buoy is marked with a red cross and the initial position of the vehicle coincides with the origin of the inertial frame. The simulation lasts 10 minutes.

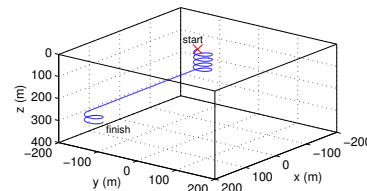


Fig. 4. Trajectory described by the vehicle

The disturbances induced by the waves in the position of the buoy are modeled using three second-order harmonic

oscillators representing the disturbance models along the x , y , and z directions,

$$H_w^i(s) = \frac{\sigma_i s}{s^2 + 2\xi_i \omega_{0i} s + \omega_{0i}^2}, \quad i = 1, 2, 3,$$

where ω_{0i} is the dominating wave frequency along each axis, ξ_i is the relative damping ratio, and σ_i is a parameter related to the wave intensity. In the simulation the dominating wave frequency was set to $\omega_{0i} = 0.8975 \text{ rad/s}$ and the relative damping ratio to $\xi_i = 0.1$. The actual position of the buoy, expressed in inertial frame coordinates, is depicted in Fig. 5. As it can be seen, the buoy wave induced random motion is confined to an interval of about 10m of height, which corresponds to extreme weather conditions.

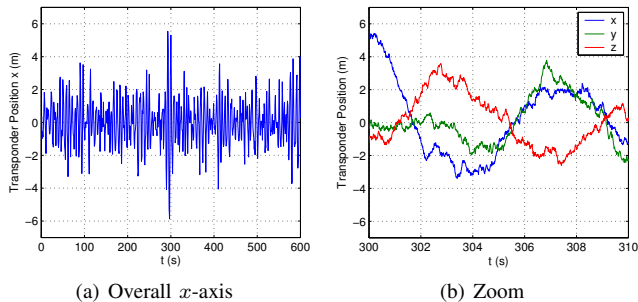


Fig. 5. Time evolution of the position of the buoy (expressed in inertial coordinates)

In the simulation the USBL measurements were corrupted by additive white Gaussian noise with standard deviation of 1 m and the measurements of the vehicle velocity relative to the water with additive Gaussian white noise with standard deviation of 0.01 m/s. In addition, the vehicle angular velocity was assumed to be corrupted by additive Gaussian noise, with standard deviation of $0.02^\circ/\text{s}$, and the attitude of the vehicle, assumed to be given by the roll, pitch, and yaw Euler angles, corrupted by additive white Gaussian noises with standard deviation of 0.03° for the roll and pitch and 0.3° for the yaw. Finally, the USBL was assumed to be operating at a frequency of 1 Hz with measurement delays modeled by an exponential distribution, with parameter $\lambda = 0.075$, and all the other sensors, which provide continuous-time signals, were sampled, in order to allow for a digital implementation of the filter, at 100Hz. The open-loop propagation of the system state estimates was carried out with the Dormand-Prince method. In order to properly tune the behavior of the filter the frequency weights were chosen as $\mathbf{W}_d = 0.01\mathbf{I}_6$ and

$$\mathbf{W}_n(s) = \frac{\sigma_1 s}{s^2 + 2\xi_1 \omega_{01} s + \omega_{01}^2},$$

with $\mathbf{L}_p = \mathbf{I}_6$, $\mathbf{M}_p = \mathbf{I}_3$, and $N_d = 1$.

The time evolution of the filter estimates is presented in Fig. 6. The position of the buoy if there were no ocean waves is also shown, as well as the actual ocean current velocity, all expressed in body-fixed coordinates. From these plots the performance of the filter is evident - only the initial transients are noticeable.

The evolution of the filter error variables is shown in Fig. 7. The initial transients arise due to the mismatch of the initial conditions of the states of the filter and can be considered as a warming up time of 3 minutes of the corresponding Integrated Navigation System. The filter error variables are shown in greater detail in Fig. 8. From the various plots it can be concluded that the disturbances induced by the waves, as well as the noise of the sensors,

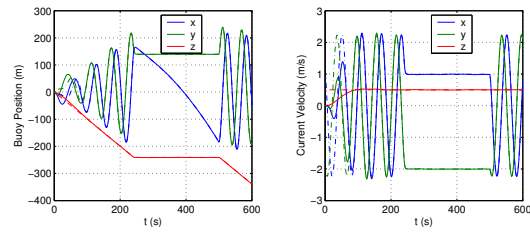


Fig. 6. Actual (dash-dot lines) and estimated (solid lines) variables

are highly attenuated by the filter, producing very accurate estimates of the velocity of the current and the position of the buoy. The delays in the position measurements are also dealt with successfully.

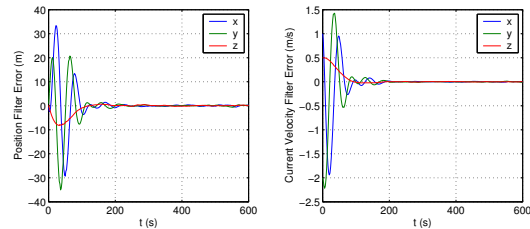


Fig. 7. Time evolution of the Kalman filter error variables

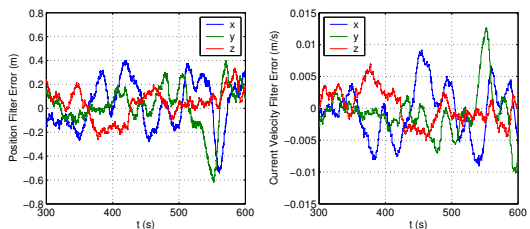


Fig. 8. Detailed evolution of the Kalman filter error variables

IV. POSITION, VELOCITY, AND ACCELERATION NAVIGATION FILTER

The navigation filter presented in the previous section addresses the specific problem of estimation of an unknown constant ocean current and, on top of that, it also yields estimates, in body-fixed coordinates, of the position of a fixed transponder in the mission scenario and the vehicle velocity. However, the latter estimate is obtained from the algebraic relation $\hat{\mathbf{v}}(t) = \mathbf{v}_r(t) + \hat{\mathbf{v}}_c(t)$, where $\mathbf{v}_r(t)$ is the relative velocity of the vehicle as measured by the Doppler sensor. Thus, the noise presented in this measure affects directly the estimate of the velocity of the vehicle $\hat{\mathbf{v}}(t)$. This section addresses this problem and a navigation filter is proposed to estimate, in body-fixed coordinates, both the velocity of the vehicle and the position of a transponder fixed in the mission scenario. Moreover, the filtering solution also accounts for the acceleration of gravity, which is of major importance in the design of navigation filters since, due to its magnitude, any misalignment in the estimate of the gravity vector leads to severe problems in the acceleration compensation. The proposed filtering framework is presented in Section IV-A, whereas simulation results are offered in Section IV-B.

A. Filtering Framework

Consider a setup similar to the one presented in Section III, where an AUV moves in a mission scenario equipped with an AHRS, which provides the attitude and angular velocity of the vehicle, an USBL sensor, which provides the position of a fixed transponder in the mission scenario, and an accelerometer, whose measurements satisfy

$$\mathbf{a} = \dot{\mathbf{v}} - \mathbf{g} + \mathbf{S}(\boldsymbol{\omega})\mathbf{v}, \quad (19)$$

where \mathbf{a} is the accelerometer measurement and \mathbf{g} denotes the gravity acceleration vector expressed in body-fixed coordinates. In order to derive the filtering solution, the derivative of the position (17) can be rewritten as

$$\dot{\mathbf{e}} = -\mathbf{v} - \mathbf{S}(\boldsymbol{\omega})\mathbf{e}. \quad (20)$$

On the other hand, from (19), it follows that

$$\dot{\mathbf{v}} = \mathbf{a} + \mathbf{g} - \mathbf{S}(\boldsymbol{\omega})\mathbf{v}. \quad (21)$$

The time derivative of \mathbf{g} is simply given by

$$\dot{\mathbf{g}} = -\mathbf{S}(\boldsymbol{\omega})\mathbf{g} \quad (22)$$

as it is constant in the inertial frame. Again, the dynamic system (20)-(22) fits in the class of systems proposed in the paper.

B. Simulation Results

To illustrate the performance of the solution proposed in the previous section the simulation presented in Section III-B was modified to fit the estimation setup presented in Section IV-A. The environmental disturbances were kept, as well as the noise on the attitude and angular velocity measurements. The acceleration measurements were corrupted by additive white Gaussian noise with standard deviation of 0.006 m/s^2 . The frequency weight \mathcal{W}_d was modified to $\mathbf{W}_d = 0.0025 \mathbf{I}_9$ to properly tune the filter.

Due to the lack of space, only the evolution of the filter error variables is shown, in Fig. 9 and, in greater detail, in Fig. 10. In comparison with the results presented in Section III-B, they are slightly worse. This is explained by the higher order of the system and the difference in the sensor suite. Nevertheless, it should be noticed that the performance attained is quite good even in the presence of extreme environmental disturbances and realistic measurements, with noise and time delays.

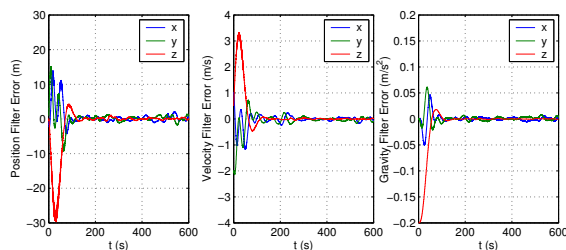


Fig. 9. Time evolution of the Kalman filter error variables

V. CONCLUSIONS

This paper presented the design and performance evaluation of a continuous-time Kalman filter with discrete-time delayed measurements for a class of time-varying kinematic systems with application to the estimation of linear motion

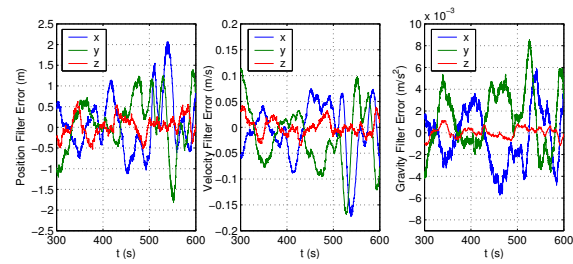


Fig. 10. Detailed evolution of the Kalman filter error variables

quantities (position, linear velocity, and acceleration of gravity), in three dimensions, of mobile platforms. The proposed technique is based on the linear time invariant Kalman filter and employs frequency weights to explicitly achieve adequate disturbance rejection and measurement noise attenuation on the state estimates. The design is optimal assuming exact angular measurements and a computationally-efficient limit filtering solution was proposed. Two practical applications were presented. In the first case study a Navigation filter was designed for the estimation of unknown constant ocean currents. In the second case the proposed solution addressed the estimation of the velocity of an underwater vehicle, as well as the acceleration of gravity. Simulation results have shown that good performance is achieved even in the presence of extreme environmental disturbances and realistic measurements, including measurement noise and delays. Other applications based on the proposed filtering design methodology can be devised for other classes of systems such as aerial, ground, and space platforms.

REFERENCES

- [1] T. Fossen and A. Grøvlen, "Nonlinear Output Feedback Control of Dynamically Positioned Ships Using Vectorial Observer Backstepping," *IEEE Trans. on Control Systems Technology*, vol. 6, no. 1, pp. 121–128, Jan. 1998.
- [2] A. Robertsson and R. Johansson, "Comments on Nonlinear Output Feedback Control of Dynamically Positioned Ships Using Vectorial Observer Backstepping," *IEEE Trans. on Control Systems Technology*, vol. 6, no. 3, pp. 439–441, May 1998.
- [3] T. I. Fossen and J. P. Strand, "Passive nonlinear observer design for ships using Lyapunov methods: full-scale experiments with a supply vessel," *Automatica*, vol. 35, no. 1, pp. 3–16, Jan. 1999.
- [4] H. Nijmeijer and T. I. Fossen (Eds), *New Directions in Nonlinear Observer Design (Lecture Notes in Control and Information Sciences)*. Springer, 1999.
- [5] A. Pascoal, I. Kaminer, and P. Oliveira, "Navigation System Design Using Time Varying Complementary Filters," *IEEE Aerospace and Electronic Systems*, vol. 36, no. 4, pp. 1099–1114, Oct. 2000.
- [6] J. E. Refsnes, A. Sørensen, and K. Y. Pettersen, "Robust observer design for underwater vehicles," in *Proc. 46th IEEE Conf. on Control Applications*, Munich, Germany, Oct. 2006.
- [7] J. C. Kinsey, R. M. Eustice, and L. L. Whitcomb, "A Survey of Underwater Vehicle Navigation: Recent Advances and New Challenges," in *Proc. 7th IFAC Conference on Manoeuvring and Control of Marine Craft (MCMC2006)*, Lisboa, Portugal, 2006.
- [8] P. G. Savage, "Strapdown Inertial Navigation Integration Algorithm Design Part 2: Velocity and Position Algorithms," *Journal of Guidance, Control, and Dynamics*, vol. 21, no. 2, pp. 208–221, Mar. 1998.
- [9] P. Batista, C. Silvestre, and P. Oliveira, "Kalman and \mathcal{H}_∞ Optimal Filtering for a Class of Kinematic Systems," in *Proc. 17th IFAC World Congress (accepted)*, Seoul, Korea, July 2008.
- [10] —, "Position and Velocity Navigation Filters for Marine Vehicles," in *Proc. 17th IFAC World Congress (accepted)*, Seoul, Korea, July 2008.
- [11] C. Silvestre, A. Aguiar, P. Oliveira, and A. Pascoal, "Control of the SIRENE Underwater Shuttle: System Design and Tests at Sea," in *Proc. 17th International Conference on Offshore Mechanics and Arctic Engineering (OMAE'98- Conference)*, July 1998.